



**HAL**  
open science

## Solvent effect on the kinetics of the hydrogenation of n-butyl levulinate to $\gamma$ -valerolactone

Sarah Capecci, Yanjun Wang, Valeria Casson Moreno, Christoph Held,  
Sébastien Leveneur

► **To cite this version:**

Sarah Capecci, Yanjun Wang, Valeria Casson Moreno, Christoph Held, Sébastien Leveneur. Solvent effect on the kinetics of the hydrogenation of n-butyl levulinate to  $\gamma$ -valerolactone. Chemical Engineering Science, 2021, 231, pp.116315. 10.1016/j.ces.2020.116315 . hal-03144830

**HAL Id: hal-03144830**

**<https://normandie-univ.hal.science/hal-03144830>**

Submitted on 6 Jan 2022

**HAL** is a multi-disciplinary open access archive for the deposit and dissemination of scientific research documents, whether they are published or not. The documents may come from teaching and research institutions in France or abroad, or from public or private research centers.

L'archive ouverte pluridisciplinaire **HAL**, est destinée au dépôt et à la diffusion de documents scientifiques de niveau recherche, publiés ou non, émanant des établissements d'enseignement et de recherche français ou étrangers, des laboratoires publics ou privés.

# Solvent effect on the kinetics of the hydrogenation of *n*-butyl levulinate to $\gamma$ -valerolactone

Sarah Capecchi<sup>1,2‡</sup>, Yanjun Wang<sup>1‡1</sup>, Valeria Casson Moreno<sup>2</sup>, Christoph Held<sup>3</sup> and Sébastien Leveneur\*<sup>1</sup>

<sup>1</sup>Normandie Univ, INSA Rouen, UNIROUEN, LSPC, EA4704, Email: sebastien.leveneur@insa-rouen.fr

<sup>2</sup>Dipartimento di Ingegneria Chimica, Civile, Ambientale e dei Materiali, Alma Mater Studiorum, Università di Bologna

<sup>3</sup>Laboratory of Thermodynamics, TU Dortmund

---

<sup>‡</sup> Authors contributed equally

## Abstract

The use of lignocellulosic biomass in the chemical industry can significantly contribute to respect the different international agreements on climate change. One of the most promising platform molecules issued from the lignocellulosic biomass hydrolysis is  $\gamma$ -valerolactone (GVL). GVL can be upgraded to different valuable chemicals, and can be produced by the hydrogenation of levulinic acid or alkyl levulinates. Although these reactions are widely studied, seldom research focused on the solvent effect. To fill this gap, the effect of three different solvents (substrate: butyl levulinate (BL); products: butanol and GVL) was studied on the kinetics of BL hydrogenation to GVL over Ru/C. PC-SAFT shows that the solubility of hydrogen is not constant during the reaction progress, and it was taken into account in the models. Kinetic models were developed using Bayesian statistics for each solvent. In the temperature range tested, the best performances are obtained when GVL is the solvent.

Keywords: Solvent effect, Kinetic modelling, PC-SAFT, Solubility,  $\gamma$ -valerolactone, Bayesian statistics

## 1. Introduction

At the present time, lignocellulosic biomass (LCB), is considered the most attractive renewable feedstock for the chemical industry, being significantly cheaper than crude oil and worldwide easily available (Ge et al., 2018). Consequently, there has been an increasing interest in developing LCB-derived platform molecules, in order to contribute to the sustainable development of the chemical industry. Indeed, major multinational companies are developing industrial processes to valorize LCB into valuable chemicals, fuels or materials (Chandel et al., 2020). Besides economic and environmental aspects, the use of LCB avoids the twenty-year ethical dilemma of “food vs. fuel” (Thompson, 2012).

The challenge in using LCB is to develop efficient and cost-effective processes and technologies for LCB pretreatment and fractionation, aimed at a full valorization of LCB components (i.e. lignin, hemicellulose, and cellulose) and to convert them to substrates for the chemical and process industry (Merklein et al., 2016).

A recent analysis showed that the bio-based product sales in 2012 were \$252 billion and renewable-based chemical sales were approximately 9% of worldwide chemical sales, being expected to grow 4% annually, and even up to 8% (from \$375 to \$441 billion) by 2020 (Takkellapati et al., 2018).

The production of platform molecules from LCB is quite significant (Dutta et al., 2012; Isikgor and Becer, 2015; Kohli et al., 2019; Luterbacher et al., 2014). There are some industrial processes for the valorization of cellulose and hemicellulose: cellulosic ethanol produced through steam explosion by Raizen company, isobutanol by Gevo company or muconic acid by Amyris company.

Among them, levulinic acid and the further upgraded molecule  $\gamma$ -valerolactone (GVL) are up-and-coming ones, showing the advantages of being stable for storage and transportation but also the reactivity for upgrading to other chemicals and fuels. In particular, due to its low vapor pressure value with temperature (Horváth et al., 2008; Pokorný et al., 2017), high flash point (96°C) and low melting point (-31°C), GVL is considered a promising solvent (Chew et al., 2020; Lin et al., 2017; Liu et al., 2020). This renewable molecule can also be used as a fuel additive instead of ethanol, which is corrosive and volatile (Alonso et al., 2013; Tang et al., 2014). GVL is also a platform molecule that can be valorized into bio-products to be used as fuels, materials and chemicals (Fig. 1).

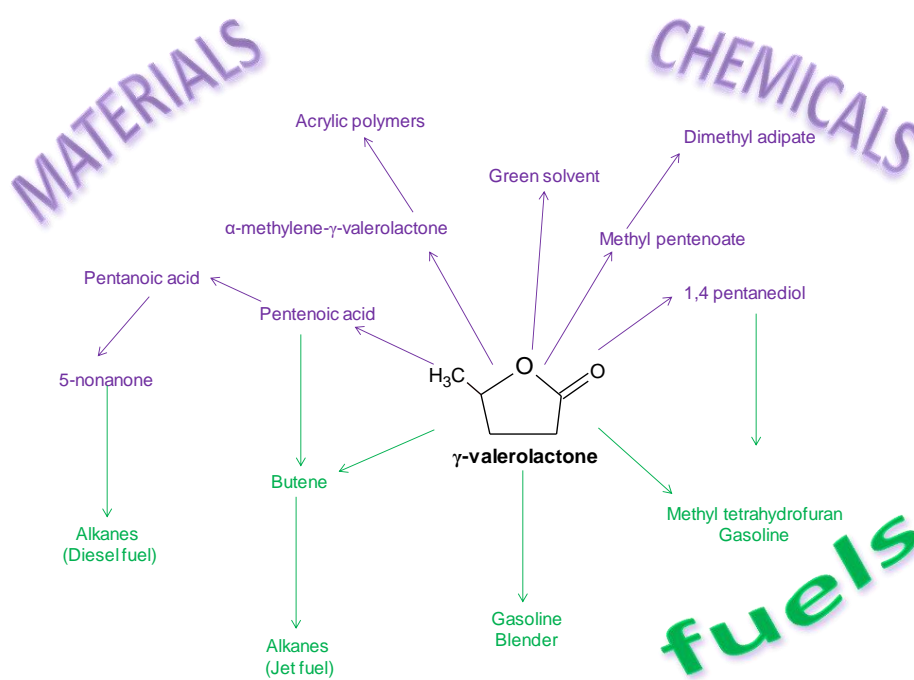


**Fig. 1.** GVL valorization into bio-products (fuels, chemicals or materials).

Among the possible routes for GVL production from LCB, one can cite three different ways for the hydrogenation of levulinic acid or alkyl levulinates: (Alonso et al., 2013; Tang et al., 2014; Yan et al., 2015) (i) use of molecular hydrogen (Al-Shaal et al., 2012; Du et al., 2013; Hengne and Rode, 2012; Luo et al., 2013; Mehdi et al., 2008; Park et al., 2015; Shimizu et al., 2014; Sudhakar et al., 2014; Testa et al., 2015); (ii) in-situ decomposition of formic acid to hydrogen (Deng et al., 2010, 2009; Du et al., 2011; Fábos et al., 2014; Fellay et al., 2008; Heeres et al., 2009; Hengne et al., 2014; Mehdi et al., 2008; Ortiz-Cervantes and García, 2013; Ruppert et al., 2016; Son et al., 2014; Yuan et al., 2013) and (iii) alcohols for catalytic transfer hydrogenation by Meerwein-Ponndorf-Verley reaction (Chia and Dumesic, 2011; Enumula et al., 2016; He et al., 2016; Kuwahara et al., 2017; Li et al., 2016a, 2016b; Song et al., 2015a, 2015b; Tang et al., 2015, 2013).

In this study, the production of GVL from molecular hydrogen was studied, which is the most efficient way (Tang et al., 2014). Several homogeneous or heterogeneous catalysts with non-noble, noble metals and miscellaneous metals have been developed to catalyze this reaction (Table 1).

**Table 1.** Hydrogenation of LA and its esters to GVL by using H<sub>2</sub> in batch reactor.

Catalyst	Temperature [°C]	P(H <sub>2</sub> ) [bar]	Solvent	Time <i>t</i> [h]	Yield at time <i>t</i> [mol%]	Ref.
Ru(acac) <sub>3</sub> +TPPTS	140	69	H <sub>2</sub> O	12	95	(Mehdi et al., 2008)
Ir/CNT	50	20	CHCl <sub>3</sub>	1	91	(Du et al., 2013)
Ni/HAP	70	5	H <sub>2</sub> O	4	65	(Sudhakar et al., 2014)
Pt/HAP	70	5	H <sub>2</sub> O	4	88	(Sudhakar et al., 2014)
Ru/HAP	70	5	H <sub>2</sub> O	4	99	(Sudhakar et al., 2014)
Ru/TiO <sub>2</sub>	130	12	Dioxane	4	92	(Luo et al., 2013)
Ru/ZSM-5	200	40	Dioxane	4	50	(Luo et al., 2013)
Cu/ZrO <sub>2</sub>	200	34.5	H <sub>2</sub> O	5	100	(Hengne and Rode, 2012)
Fe/C	170	5	H <sub>2</sub> O	3	99	(Park et al., 2015)
Ni-MoO <sub>x</sub> /C	140	8	--	5	97	(Shimizu et al., 2014)
Ni-MoO <sub>x</sub> /C	140	8	H <sub>2</sub> O	5	2	(Shimizu et al., 2014)
Pd/HMS	160	150	H <sub>2</sub> O	6	89	(Testa et al., 2015)
Ru/C	130	12	Methanol	2.67	84	(Al-Shaal et al., 2012)
Ru/C	130	12	H <sub>2</sub> O	2.67	86	(Al-Shaal et al., 2012)

Ru catalyst was found to be one of the most active and selective for GVL synthesis (Manzer, 2004). Hence, several studies in Ru catalyst with different support such as carbon, TiO<sub>2</sub>, zeolites, etc. were carried out. For example, Ru supported on hydroxyapatite catalyst demonstrated higher activity and selectivity than Pt, Pd and Ni for hydrogenation of LA at low pressure and temperature (Sudhakar et al., 2014). However, the supports of Ru-catalysts and solvents also have significant effects on the hydrogenation of LA (Luo et al., 2013). Non-acidic supports favor a high yield of GVL, while the zeolite-supported acidic catalysts can directly convert LA to pentanoic acid in dioxane under mild conditions. Besides, deactivation of catalyst due to the loss of acid sites by dealumination limits the reuse of catalyst.

In this study, the catalyst Ru/C was used because it is one of the most efficient (Wright and Palkovits, 2012). The production of GVL from the hydrogenation of alkyl levulinates or LA over Ru/C is a two-step reaction (Fig. 2). In the first step, hydrogenation of LA or

its esters with H<sub>2</sub> to intermediate is catalyzed by Ru/C. In the second step, intracyclization of intermediate occurs to form GVL. The second step can be catalyzed by the presence of protons from levulinic acid dissociation, solvent or catalyst.

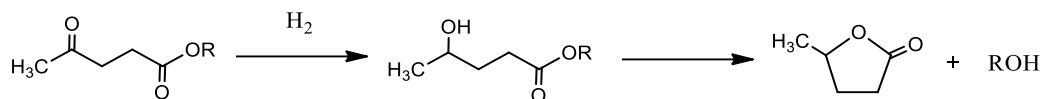


**Fig. 2.** Possible mechanism of hydrogenation of LA and its esters with H<sub>2</sub> to GVL.

The role of solvent in biomass valorization plays an important role (Altuntepe et al., 2017; Shuai and Luterbacher, 2016). The solvent choice can have an effect on the hydrogen solubility and also on the cyclization step by favoring or not the protons mobility.

Some studies have investigated the solvent effect of this reaction.

Luo et al. (2013) studied the effect of dioxane and 2-ethylhexanoic acid solvents on the hydrogenation of levulinic acid over Ru-based catalysts. They showed that the 2-ethylhexanoic solvent is more stable under the operating conditions, and has a similar acidity constant with respect to levulinic acid.

Kasar et al. (2018) studied the effect of different alcohol solvents (methanol, 2-propanol and n-butanol) and water solvent on the hydrogenation of levulinic acid over Co/La<sub>2</sub>O<sub>3</sub> catalyst. They showed that the water solvent causes the highest GVL selectivity in the water solvent, but not the highest conversion. They stated that the solvent with the bulkier group decreases the kinetics of the whole process.

Feng et al. (2020) also showed that the GVL selectivity is optimal in water solvent (compared to ethanol or 2-propanol) for the hydrogenation of ethyl levulinate over Fe-Mo<sub>2</sub>C-1:18.

Xu et al. (2019) studied the effect of methanol, ethanol, isopropanol, and dioxane solvent on the hydrogenation of levulinic acid over Ni/C-500 catalyst. They observed that GVL was mainly produced in dioxane and isopropanol solvents. The hydrogenation of levulinic acid in methanol and ethanol also leads to methyl and ethyl levulinates.

Hengst et al. (2015) studied the effect of different alcohols as solvents on conversion and selectivity for the hydrogenation of LA over 15 wt% Ni/ $\gamma$ -Al<sub>2</sub>O<sub>3</sub>. From their experiments, 1-propanol is an adequate solvent. They also found that the solvent-free reaction gives attractive results.

It was also found that GVL is a suitable solvent for this reaction in terms of kinetics (Qi and Horváth, 2012; Wettstein et al., 2012).

Despite the flourishing literature on the solvent effect for this reaction system, in some investigations, the side esterification or transesterification reaction was not taken into account. Also, the solubility of hydrogen was never discussed, and kinetic models were developed in these references (Feng et al., 2020; Hengst et al., 2015; Kasar et al., 2018; Luo et al., 2013; Qi and Horváth, 2012; Wettstein et al., 2012; Xu et al., 2019).

To avoid the separation complexity, three scenarios are interesting to evaluate: solvent-free by just using the substrate, GVL solvent and the corresponding alcohol solvent. To evaluate the effect of these solvents on the reaction kinetics, a fair comparison should be performed by developing a kinetic model for each solvent, which includes the hydrogen solubility. In the present work, the solvent effect on the kinetics of butyl levulinate hydrogenation to GVL over Ru/C was investigated. Three systems were compared: solvent-free, i.e., hydrogenation in pure BL solution, 1-butanol solvent and GVL solvent.

In the first part, the vapor pressure of these solvents with temperature was discussed. Then, the solubility of hydrogen as a function of temperature and reaction composition was estimated by the PC-SAFT equation of state. A kinetic model for each solvent was developed by using Bayesian statistics.

## 2. Experimental section

### 2.1 Chemicals

The following chemicals were used without further purification:  $\gamma$ -valerolactone (wt%  $\geq$  99%) was purchased from Sigma Aldrich. Ru/C catalyst (Ruthenium, 5% on activated carbon powder, standard, reduced, nominally 50% water wet); N-Butyl levulinate (wt%  $\geq$  98%) and Butan-1-ol (wt%  $\geq$  98%) were obtained from Alfa Aesar. Hydrogen gas (H<sub>2</sub> purity > 99,999 vol%) was from Linde. Acetone (analytical grade) was bought from VWR. Furfural was supplied by Acros Organics.

### 2.2 Analytical methods

The GC-FID was used to analyze the concentration of n-butyl levulinate and intermediate products. The apparatus is Bruker Scion GC436 equipped with flame ionization detector, an autosampler and capillary column (Rxi-5 ms, 30 m x 0.32 mm internal diameter x 0.25  $\mu$ m film thickness). Helium (99.99%) is the carrier gas used at a constant flow rate of 1.2 mL.min<sup>-1</sup> to transfer the sample from the injector, through the column and into the FID-detector. The temperature of the injector and the detector was set at 270°C. The oven temperature was provided at 35°C (3 min) - 15°C min<sup>-1</sup> - 300°C. The injection volume was 5  $\mu$ L, and the split ratio was 30:1. Furfural was used as an internal standard.

### 2.3 Kinetic experiments

The hydrogenation reaction was performed under isothermal and isobaric conditions in a 300 mL stainless steel batch Parr reactor equipped with an electrically heating jacket and a cooling coil (Fig. 3). A thermocouple measured the reaction temperature. A vigorous gas-liquid-solid mixing was ensured by a gas entrainment stirrer.

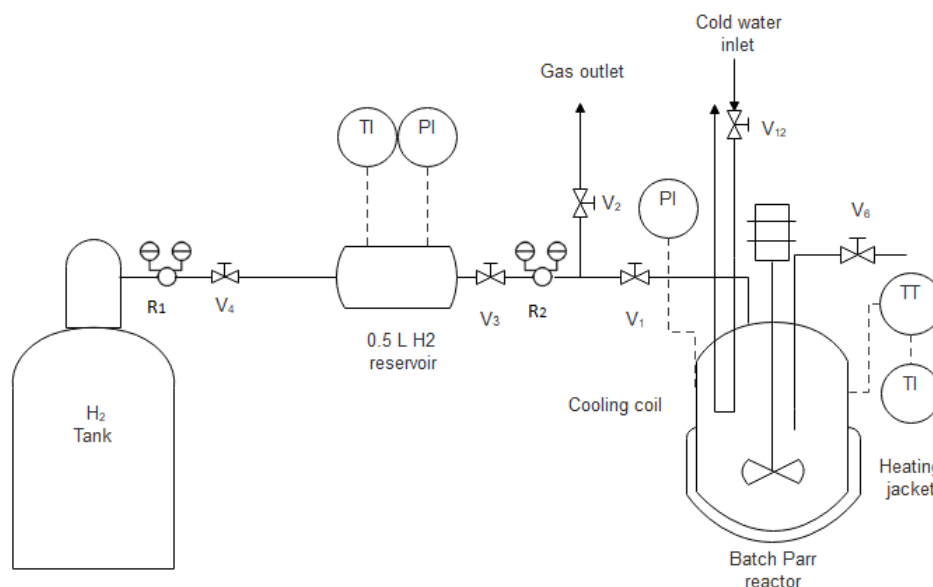


**Fig. 3.** Experimental setup of the autoclave.

The desired amount of reaction mixture and catalyst were loaded into the reactor, and then the reactor was sealed. A vacuum pump removed air from the reactor. The temperature was set at the desired value, and the agitation speed was fixed to 400 rpm to homogenize the temperature. When the temperature reached the desired value, valve  $V_1$  was opened to allow the gas to go into the reactor, and the agitation rate was set to 1000 rpm. In this way, the three different phases inside the reactor vessel were well mixed, and the reaction started. In previous work, it was found that external and internal liquid-solid mass transfer can be neglected under this operating condition (Wang et al., 2019).

During the reaction, at different times, samples were withdrawn through valve  $V_6$ . The samples were filtered by a syringe to separate the liquid reaction mixture from the catalyst Ru/C. Tables 2-4 show the experimental matrix with the operating conditions.

**Table 2.** Experimental matrix in GVL solvent (Isothermal & isobaric conditions).

Exp. number	P <sub>H2</sub> [bar]	Temp [°C]	mcat_wet_basis [kg]	m <sub>0</sub> (GVL) [kg]	m <sub>0</sub> (BL) [kg]	C <sub>BL0</sub> [mol L <sup>-1</sup> ]	C <sub>Int0</sub> [mol L <sup>-1</sup> ]	C <sub>GVLO</sub> [mol L <sup>-1</sup> ]	C <sub>BuOH0</sub> [mol L <sup>-1</sup> ]
1	20	120	0.001	0.0812	0.0413	1.84	0.00	6.8	0.0
2	20	100	0.001	0.0812	0.0413	1.76	0.00	6.69	0.0
3	20	100	0.0005	0.0812	0.0413	1.82	0.00	6.85	0.0

**Table 3.** Experimental matrix in BL solvent (Isothermal & isobaric conditions).

Exp. number	P <sub>H2</sub> [bar]	Temp [°C]	mcat_wet_basis [kg]	m <sub>0</sub> (GVL) [kg]	m <sub>0</sub> (BL) [kg]	C <sub>BL0</sub> [mol L <sup>-1</sup> ]	C <sub>Int0</sub> [mol L <sup>-1</sup> ]	C <sub>GVLO</sub> [mol L <sup>-1</sup> ]	C <sub>BuOH0</sub> [mol L <sup>-1</sup> ]
4	20	100	0.001	0.00	0.117	5.95	0.00	0.00	0.00
5	20	110	0.001	0.00	0.12	5.95	0.00	0.00	0.00

**Table 4.** Experimental matrix in butanol solvent (Isothermal & isobaric conditions).

Exp. number	P <sub>H2</sub> [bar]	Temp [°C]	mcat_wet_basis [kg]	m <sub>0</sub> (GVL) [kg]	m <sub>0</sub> (BL) [kg]	C <sub>BL0</sub> [mol L <sup>-1</sup> ]	C <sub>Int0</sub> [mol L <sup>-1</sup> ]	C <sub>GVLO</sub> [mol L <sup>-1</sup> ]	C <sub>BuOH0</sub> [mol L <sup>-1</sup> ]
6	20	100	0.001	0.06	0.04	1.98	0.00	0.00	6.59
7	20	100	0.0005	0.06	0.04	2.02	0.00	0.00	6.59
8	20	110	0.001	0.06	0.04	1.95	0.00	0.00	6.52

### **3. Results and discussion**

#### **3.1 Vapor pressure**

The vapor pressure of the solvent governs the choice of the reaction temperature, and thus the reaction kinetics. A high vapor pressure value can lower the reaction volume, and thus interfere with the kinetics of the reaction. The variation of butanol vapor pressure from 100°C to 195°C was measured by Safarov et al. (2015) The vapor pressure evolution for BL and GVL with temperature was evaluated by Aspen Plus. As suggested by Ariba et al. (2020), the Benedict–Webb–Rubin–Starling virial equation of state was used to calculate the vapor pressure values of BL and GVL between 100°C and 195°C. PC-SAFT was also used to estimate the vapor pressure evolution with temperature. The PC-SAFT methodology and use are described in the subsequent chapter. Fig. 4 shows the evolution of the vapor pressure of the three solvents with temperature.

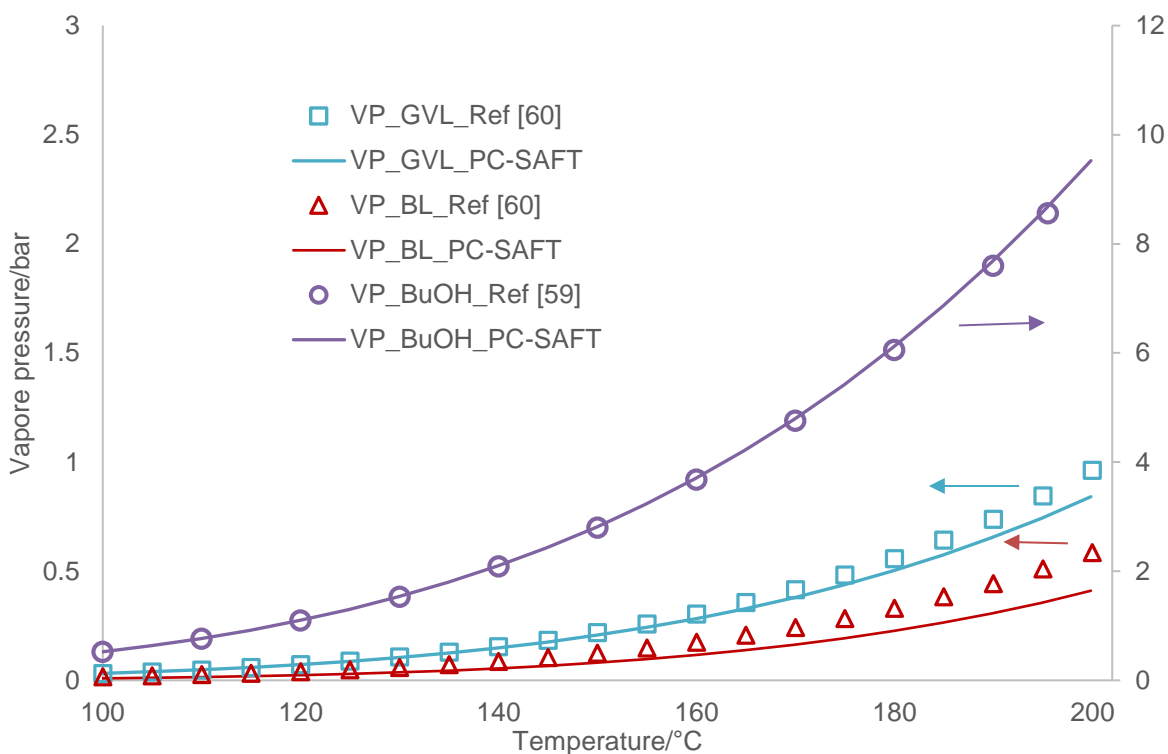


**Fig. 4.** Vapor pressures of GVL, BL and BuOH obtained from references 59 and 60; and from PC-SAFT modeling using the parameters from Table 5.

Hydrogenation of alkyl levulinate over Ru/C is usually performed within the temperature range of 100-180°C. Fig. 4 shows that the evaporation of BL and GVL can be assumed to be negligible in this temperature range. This observation is not the case when butanol is used as a solvent. Based on these results, experiments were performed in the temperature range 100-120°C to limit the effect of evaporation. The experimental matrix for each solvent is displayed by Tables 2-4 in the experimental section.

### 3.2 Solvent effect on the kinetics

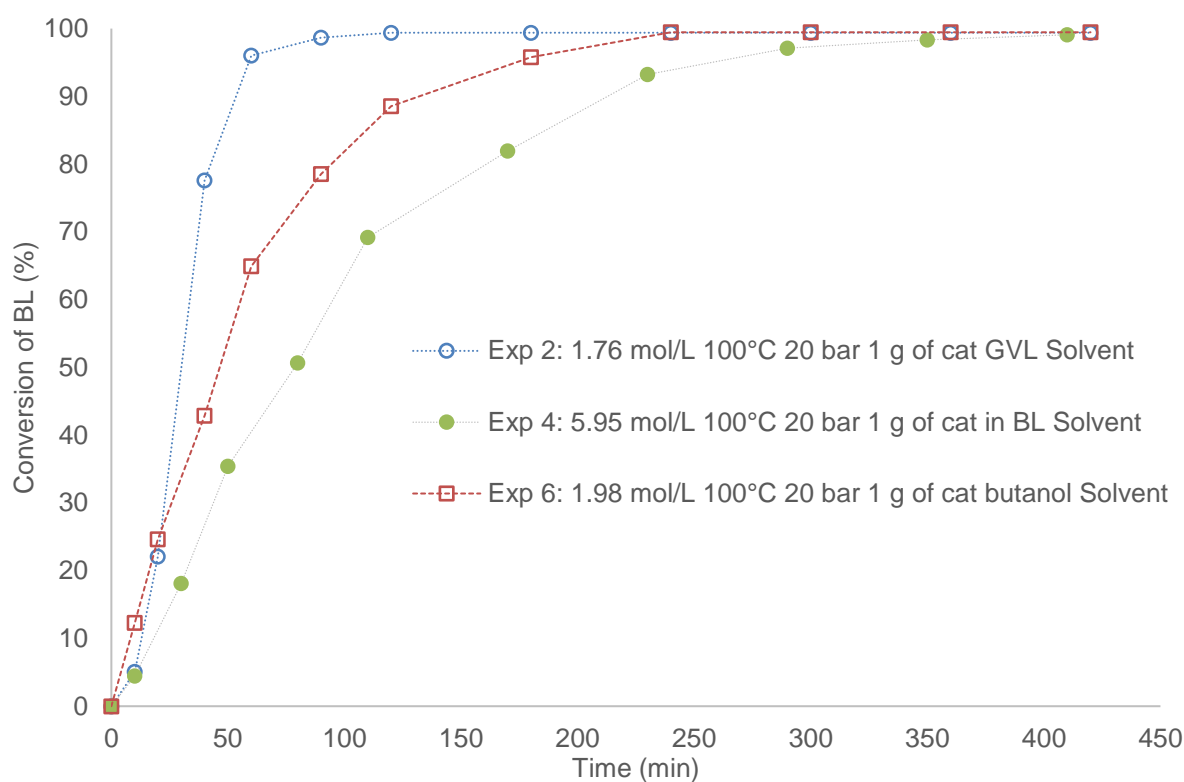
To compare the solvent effect on the reaction kinetics, experiments were carried at 100°C, 20 bar of hydrogen and with 1 gram of wet catalyst (Exps 2, 4 and 6 Tables 2-4). Clearly enough, initial BL concentration was the same for experiments using GVL and BuOH as solvents, but not for the one using BL as a solvent.

As discussed in the introduction section, there are two consecutive reactions. Thus, the conversion of BL and the GVL yield needs to be compared. The BL conversion and GVL yield were calculated as

$$\text{BL conversion}/\% = \frac{[BL]_0 - [BL]}{[BL]_0} * 100 \quad (1)$$

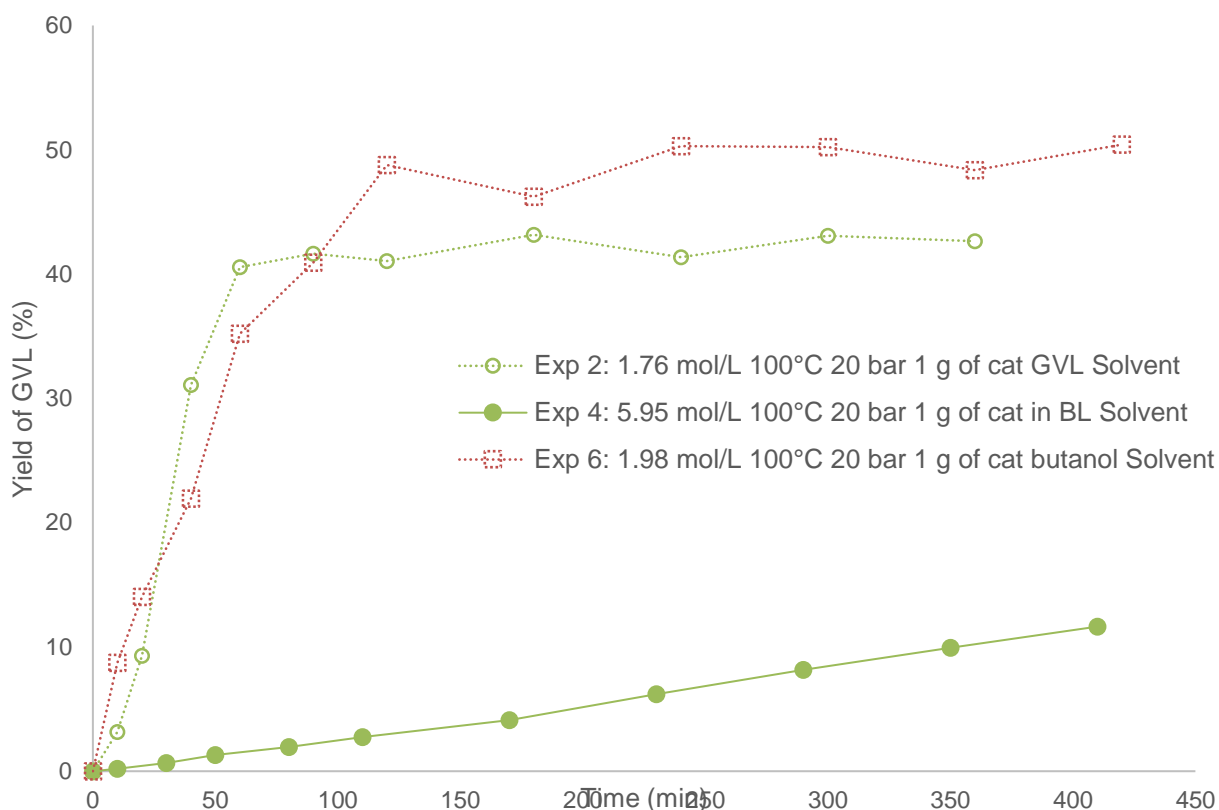
$$\text{Yield of GVL}/\% = \frac{\text{Concentration of GVL produced}}{[BL]_0} * 100 \quad (2)$$

Fig. 5 shows the solvent effect on the kinetics of the hydrogenation step.



**Fig. 5.** Solvent effect on the kinetics of BL conversion for Exps 2; 4 and 6: isothermal conditions at 100°C and isobaric conditions at 20 bars.

Fig. 5 shows that the kinetics of hydrogenation follows the order:  $R_{\text{Hydrogenation/GVL}} > R_{\text{Hydrogenation/BuOH}} > R_{\text{Hydrogenation/BL}}$ , where  $R_{\text{Hydrogenation/Solvent}}$  is the rate of hydrogenation. One can notice that until 20 minutes, the kinetics is similar for the hydrogenation step in BuOH and GVL solvent. This difference of kinetics can be explained by hydrogen solubility, competition on the active catalyst site, or the solvation effect.



**Fig. 6.** Solvent effect on the kinetics of GVL yield for Exps 2; 6 and 4: isothermal conditions at 100°C and isobaric conditions at 20 bars.

Fig. 6 shows the kinetics of the second reaction step, i.e., cyclization. The kinetics in GVL and butanol solvents are similar for the cyclization. However, the cyclization in the BL solvent is slower compared to the one in BuOH or GVL. The kinetics of the second reaction is not linked to hydrogen pressure or catalyst loading (Wang et al., 2019). Thus, the intermediate is more stable in BL solvent than in BuOH or GVL solvents. The

development of kinetic models for these three scenarii requires the knowledge of hydrogen solubility and its variation with the chemical composition and temperature.

### 3.3 PC-SAFT modeling

Modeling the vapor pressure of pure components is realized by a vapor-liquid equilibrium condition. For pure-components, the fugacity coefficient, which describes the deviation from the ideal-gas behavior, of the component in the vapor phase ( $\varphi_{0i}^V$ ) needs to be equal to the fugacity coefficient of the pure component in the liquid phase  $\varphi_{0i}^L$ . The following relation was applied in this work to describe the vapor-liquid equilibrium of a pure component:

$$1 - \frac{\varphi_{0i}^L}{\varphi_{0i}^V} < 10^{-8} \quad (3)$$

Modeling gas solubility in any solvent or solvent mixture is realized by a vapor-liquid equilibrium condition. At high-pressure conditions, an equation of state is required that allows solving the isofugacity criterion, which must be fulfilled for each component  $i$  in equation (4) that is present in the two phases (liquid, L and vapor, V):

$$\varphi_i^L \cdot x_i = \varphi_i^V \cdot y_i \quad (4)$$

In this equation,  $y_i$  denotes the mole fraction of the component  $i$  in the vapor phase. The equation is solved iteratively in order to finally obtain the solubility of the gas in the liquid phase, i.e.  $x_i$ . In this work, the hydrogen solubility in pure solvents and solvent mixtures is modeled, and the fugacity coefficients were predicted with PC-SAFT by using the following equation:

$$\ln(\varphi_i) = \frac{\mu_i^{res}}{k_B \cdot T} - \ln \left( 1 + \left( \frac{\partial \left( \frac{a^{res}}{k_B \cdot T} \right)}{\partial \rho} \right) \right) \quad (5)$$

Here,  $k_B$  and  $T$  are the Boltzmann constant and the temperature in Kelvin, and  $\mu_i^{res}$ ,  $\rho$  and  $a^{res}$  denote the residual chemical potential, reduced density, and residual Helmholtz energy, respectively. In this work, classical PC-SAFT (Gross and Sadowski, 2001) was used that accounts for three independent contributions to the residual Helmholtz energy  $a^{res}$ :

$$a^{res} = a^{hc} + a^{disp} + a^{assoc} \quad (6)$$

These independent contributions are  $a^{hc}$  (hard-chain contribution),  $a^{disp}$  (dispersion contribution),  $a^{assoc}$  (association contribution). Such expressions are available in the original PC-SAFT publication, and require the availability of pure-component parameters: the segment number  $m_{seg}$ , the segment diameter  $\sigma_i$ , dispersion-energy parameter  $u_i/k_B$  and two association parameters  $\varepsilon^{AiBi}$  (association-energy parameter) and  $\kappa^{AiBi}$  (association-volume parameter). The 2B association scheme that mimics the number of hydrogen-bond donors  $A_i$  and acceptors  $B_i$  was applied in this work to 1-butanol. All other components were treated as non-associating, i.e., these can neither form self-associations nor cross-associations. Such parameters are available for the components considered in this work, according to Table 5. The parameters allow satisfactorily modeling the vapor pressures of 1-butanol, GVL, and BL, which is illustrated in Fig. 4. Besides, one can notice a good agreement between vapor pressure determined from references (Ariba et al., 2020; Safarov et al., 2015), and the ones estimated by the PC-SAFT method.

**Table 5.** PC-SAFT pure-component parameters for the components considered in this work.

Parameter	H <sub>2</sub>	1-Butanol	GVL	BL
$m_{\text{seg}}$ [-]	1.306	2.7515	2.8892	5.3007
$\sigma$ [Å]	2.601	3.6139	3.6208	3.5910
$u_i/k_B$ [K]	23.42	259.59	362.6	265.1504
N [-]	-	1:1	-	-
$\frac{\epsilon^{A_i B_i}}{k_B}$ [K]	-	2544.6	-	-
$\kappa^{A_i B_i}$ [-]	-	0.006692	-	-
Ref.	(Thi et al., 2006)	(Gross and Sadowski, 2002)	(Klajmon et al., 2015)	(Altuntepe et al., 2017)

Based on the pure-component parameters from Table 5, the solubility of H<sub>2</sub> in the single solvents 1-butanol, GVL, and BL was modeled using the isofugacity criterion. Modeling mixtures require combining and mixing rules. Therefore, Berthelot-Lorenz combining rules (Berthelot, 1898; Lorentz, 1881) were incorporated into PC-SAFT as follows:

$$\sigma_{ij} = \frac{1}{2}(\sigma_i + \sigma_j) \quad (7)$$

$$u_{ij} = \sqrt{u_i u_j}(1 - k_{ij}(T)) \quad (8)$$

The binary  $k_{ij}$  parameters have been used according to Table 6.

**Table 6.**  $k_{ij}$  parameters determined in this work or set to zero.

Binary pair	$k_{ij}$
H <sub>2</sub> – 1-Butanol	$-0.00158 \cdot T + 0.24$
H <sub>2</sub> – GVL	-
H <sub>2</sub> – BL	-

It can be observed from Table 6 that only for the mixture H<sub>2</sub>-1-butanol  $k_{ij}$  parameters were used. The fitted values for the pair H<sub>2</sub>-1-butanol are valid in the temperature range 295 - 525 K, only valid with the pure-component parameters in Table 5. A  $k_{ij}$  parameter was not required for the mixture H<sub>2</sub>-GVL as PC-SAFT allowed for a reasonable prediction ( $k_{ij} = 0$ ) for the H<sub>2</sub> solubility in GVL. Further, the  $k_{ij}$  parameter was set to zero for the mixture H<sub>2</sub>-BL as experimental data was not available for this mixture. The result of the PC-SAFT modeled H<sub>2</sub> solubility in the single solvents is illustrated in Fig. 7 at 20 bar between 100°C and 150°C, respectively. The H<sub>2</sub> solubility increases in the order  $x_{H_2}(\text{in GVL}) < x_{H_2}(\text{in BL}) < x_{H_2}(\text{in 1-butanol})$ . In all solvents,  $x_{H_2}$  increases with temperature, which is a special characteristic of H<sub>2</sub> compared to other gases that show the regular behavior that gas solubility decreases with increasing temperature. This can be predicted with PC-SAFT reasonably. Please note that the  $k_{ij}$  parameters between H<sub>2</sub> and 1-butanol were fitted in this work to data at pressures between 40 bar and 80 bar, while Fig. 7 shows the solubility at 20 bar. Thus, due to a lack of data at 20 bar it is not possible to validate PC-SAFT modeled H<sub>2</sub> solubility in 1-butanol at 20 bar. Based on the pure-component parameters and the binary  $k_{ij}$  parameters, PC-SAFT was applied to predict the H<sub>2</sub> solubility in solvent mixtures at various conditions.

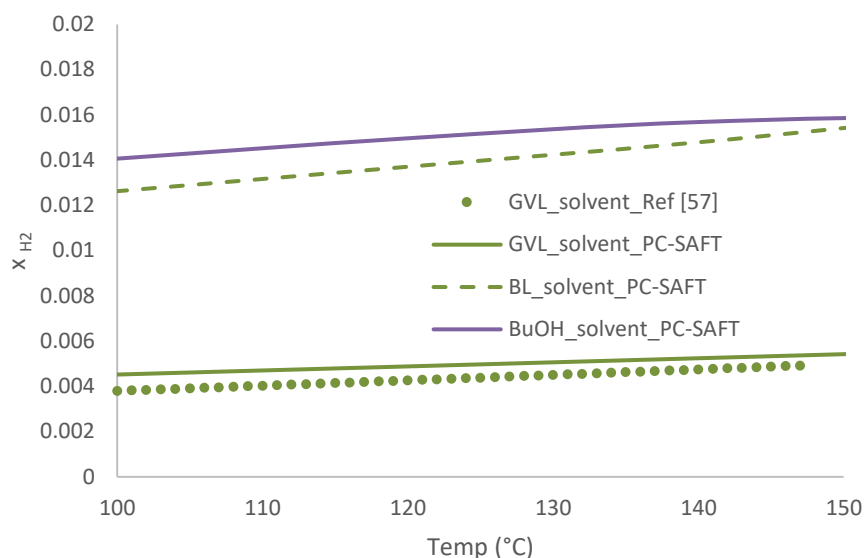


**Fig. 7.** H<sub>2</sub> solubility in GVL solvent, in BL solvent, and in 1-butanol solvent at isobaric conditions at 20 bars.

One can notice that the rate of hydrogenation and hydrogen solubility in the solvent do not evolve in the same way. Indeed, the rate of BL hydrogenation evolves in the following order:  $R_{\text{Hydrogenation/GVL}} > R_{\text{Hydrogenation/BuOH}} > R_{\text{Hydrogenation/BL}}$ , and the solubility of hydrogen evolves in the following order:  $x_{\text{H}_2}(\text{in 1-butanol}) > x_{\text{H}_2}(\text{in BL}) > x_{\text{H}_2}(\text{in GVL})$ . As mentioned earlier, the rates of hydrogenation in butanol and GVL are similar during the first 20 minutes. Fig. S1 shows the evolution of the concentration of hydrogen in the liquid phase along the reaction time for experiments 2, 4 and 6. One can notice that the solubility of hydrogen is higher in BL solvent during the reaction than in the other solvents. The fact that the rate of hydrogenation in BL is the slowest one despite the fact that the solubility in this solvent is higher could be explained by surface reaction competition. The use of PC-SAFT demonstrates that hydrogen solubility does not explain the solvent-induced difference of kinetics. The difference of reactivity is linked to the kinetics, and particularly the activation energies and rate constants. Hence, kinetic models are needed to estimate these kinetic constants.

### 3.4 Kinetic modeling

Several studies (Negahdar et al., 2017; Piskun et al., 2016; Wang et al., 2019) have shown that the rate expression for the hydrogenation of alkyl levulinates over Ru/C can be expressed by a power-law. The kinetic expression for the hydrogenation step was expressed as:

$$R_{Hydrogenation} = R_1 = k_1 * C_{BL} * C_{H_2} * \omega_{cat} \text{ (kg of dry basis catalyst per L of reaction mixture)} \quad (9)$$

The concentration of hydrogen was estimated from the PC-SAFT method.

For the cyclization step, the kinetic expression in GVL and BL was expressed as:

$$R_{Cyclization} = R_2 = k_2 * C_{Int} \quad (10)$$

Based on the experimental data, the reverse reaction for the cyclization step in butanol solvent cannot be neglected. Hence, the kinetic expression was expressed as

$$R_{Cyclisation} = R_2 = k_2 * \left( C_{Int} - \frac{1}{K} * C_{GVL} * C_{BuOH} \right) \quad (11)$$

The kinetics of mass transfer can be considered to be fast compared to the kinetic reaction (Wang et al., 2019). The material balances were derived as:

$$\frac{dC_{BL}}{dt} = -R_1 \quad (12)$$

$$\frac{dC_{Int}}{dt} = R_1 - R_2 \quad (13)$$

$$\frac{dC_{GVL}}{dt} = R_2 \quad (14)$$

$$\frac{dC_{BuOH}}{dt} = R_2 \quad (15)$$

Athena Visual Studio® v14.2 was used to estimate the kinetic and equilibrium constants (Stewart and Caracotsios, 2010, 2008). This software uses the Bayesian estimation method for non-linear regressions. The DDALPUS algorithm solved the ordinary differential Equations (12)-(15) (Caracotsios and Stewart, 1985). The GREGLUS package, using a Bayesian estimator, can provide optimal parameter estimates and 95% confidence intervals. This package provides the normalized parameter covariance matrix.

During the parameter estimation, the GREGPLUS package minimizes the objective function  $S(\theta)$ , and can calculate the maximum posterior probability density of the different estimated parameters  $\theta$  and the values of the posterior distribution of the tested models (Stewart and Caracotsios, 2010, 2008).

$$S(\theta) = (n + m + 1) \cdot \ln|v(\theta)| \quad (16)$$

With,  $n$  is the number of events in response,  $m$  is the number of responses, and the term  $|v(\theta)|$  is the determinant of the covariance matrix of the responses. Each element of this matrix is defined as

$$v_{ij}(\theta) = \sum_{u=1}^n [Y_{iu} - f_{iu}(\xi_u, \theta)] \cdot [Y_{ju} - f_{ju}(\xi_u, \theta)] \quad (17)$$

With  $Y_{iu}$  the experimental concentration and  $f_{iu}(\xi_u, \theta)$  the estimated value for the response  $i$  and event  $u$ ;  $Y_{ju}$  the experimental concentration and  $f_{ju}(\xi_u, \theta)$  the estimated value for response  $j$  and event  $u$ .

To avoid the correlation between the pre-exponential factor and activation energy, a modified Arrhenius equation was used to express the rate constants

$$k_1(T) = k_1(T = 378.15K) \cdot \exp\left(\frac{-E_{a1}}{R} \cdot \left(\frac{1}{T} - \frac{1}{378.15}\right)\right) \quad (18)$$

$$k_2(T) = k_2(T = 378.15K) \cdot \exp\left(\frac{-E_{a2}}{R} \cdot \left(\frac{1}{T} - \frac{1}{378.15}\right)\right) \quad (19)$$

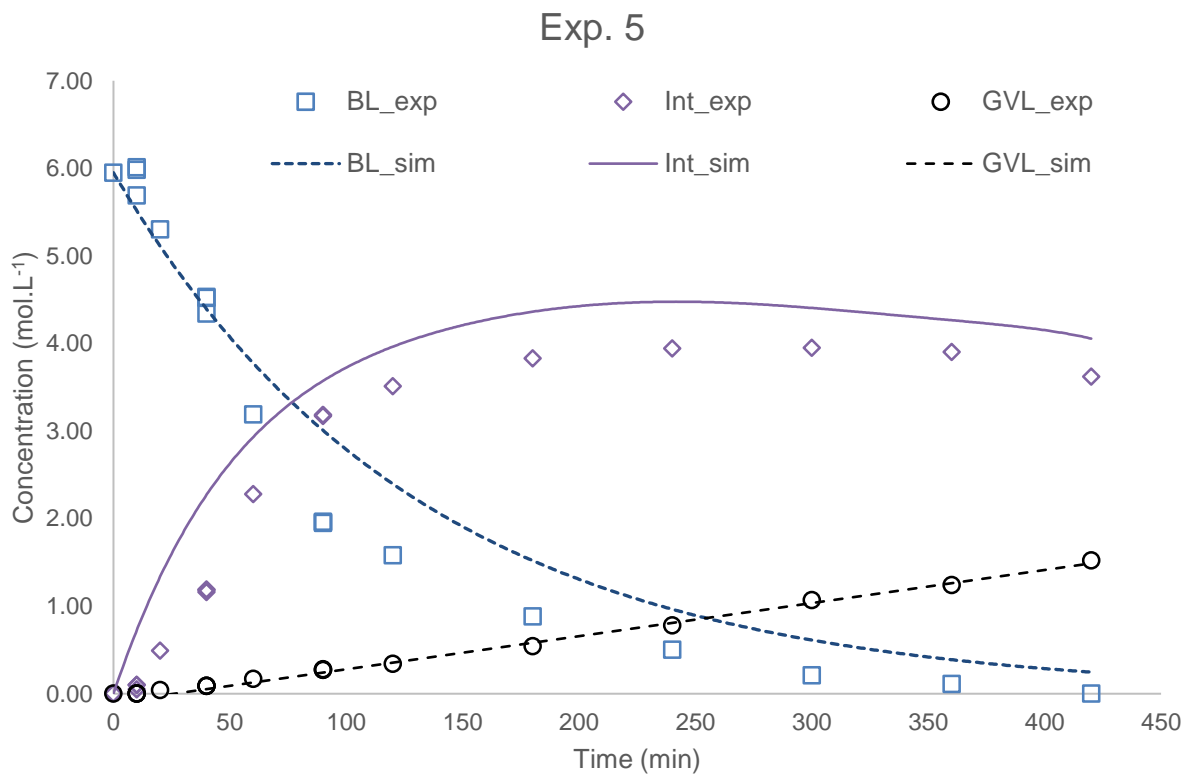
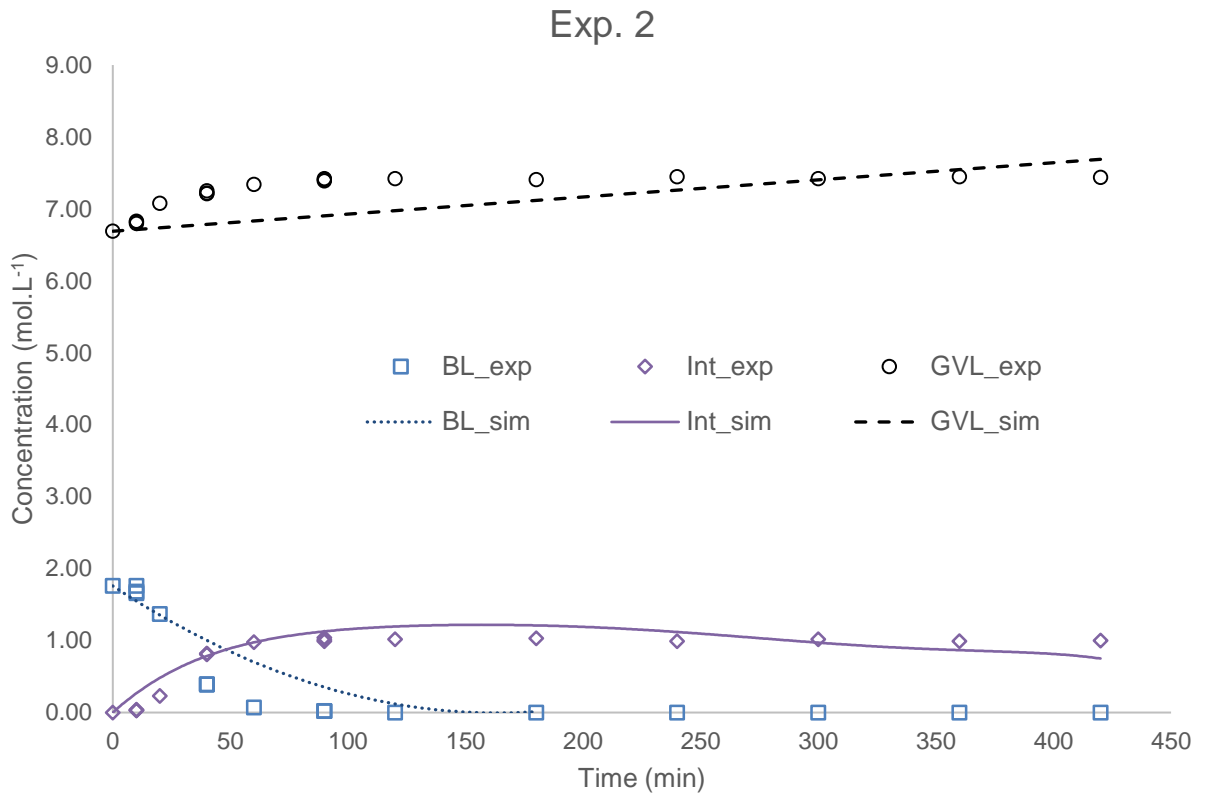
Due to the narrow temperature range (100-120°C), the equilibrium constant K can be assumed to be temperature independent.

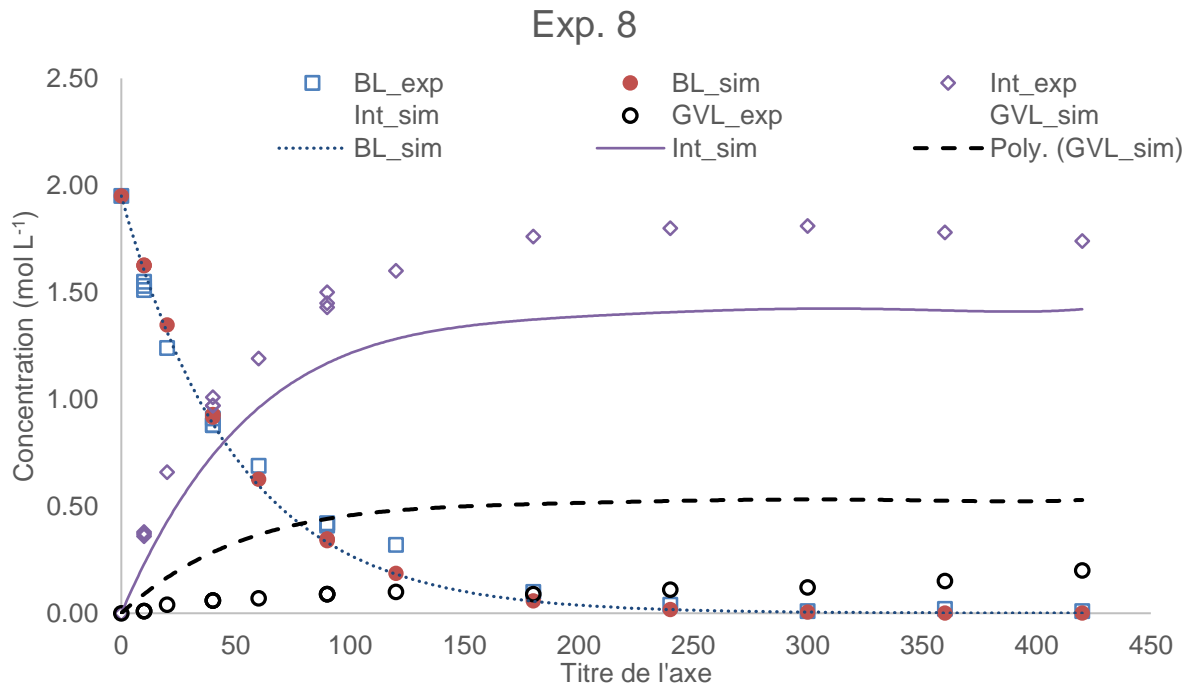
The kinetic constants ( $k_1(T = 378.15K)$ ,  $E_{a1}$ ,  $k_2(T = 378.15K)$  and  $E_{a2}$ ) were estimated for each solvent (Tables 2-4). For the hydrogenation in butanol solvent, the equilibrium constant was estimated. The concentrations of BL, intermediate and GVL were used as observables during the regression.

Fig. 8 shows the fit of the models to the experimental concentration for some experiments. In general, the models fit the experimental data, as confirmed by parity plots (Fig. S2). To evaluate the quality of the three models, F-test of overall significance was carried out. It was found that the three models were significant at 99%.

The developed models in GVL and BL solvents have a slight tendency to underestimate BL concentrations (Fig. 8, Exps 2&5). The developed model in butanol solvent tends to underestimate intermediate concentrations (Fig. 8, Exp. 8). The fact that the models underestimate some concentrations might be linked to surface reactions that are not taken into account.

Table 7 displays the values of estimated parameters and their confidence interval. The confidence interval values (Table 7) and the covariance matrix (Tables S1-S3) show that the parameters are well estimated. The correlations between the estimated parameters vary from low to medium showing good reliability of the developed models.



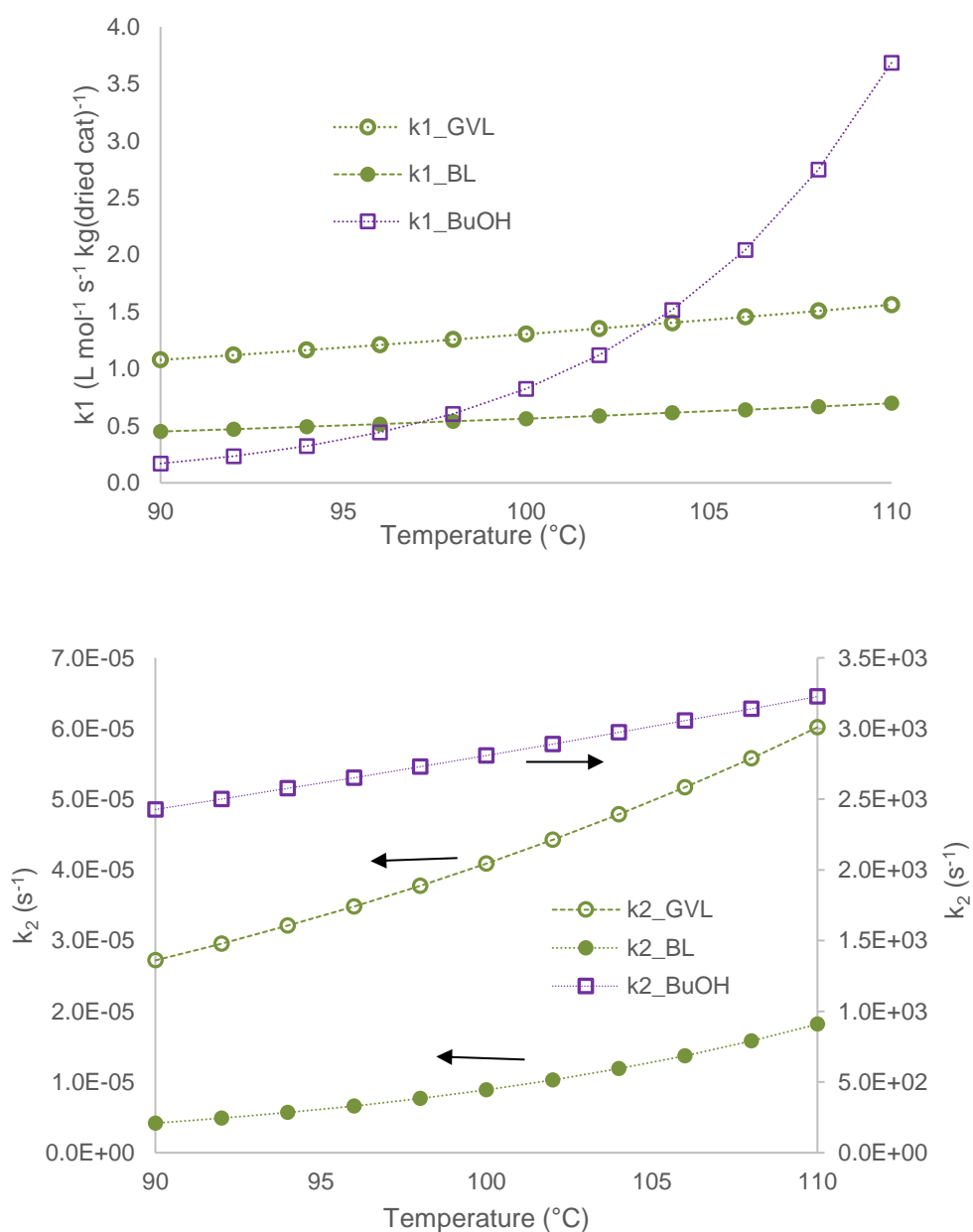


**Fig. 8.** Fit of the model to the experimental data Exps 2, 5 and 8.

**Table 7.** Parameter estimation: estimated parameters with their 95% confidence intervals.

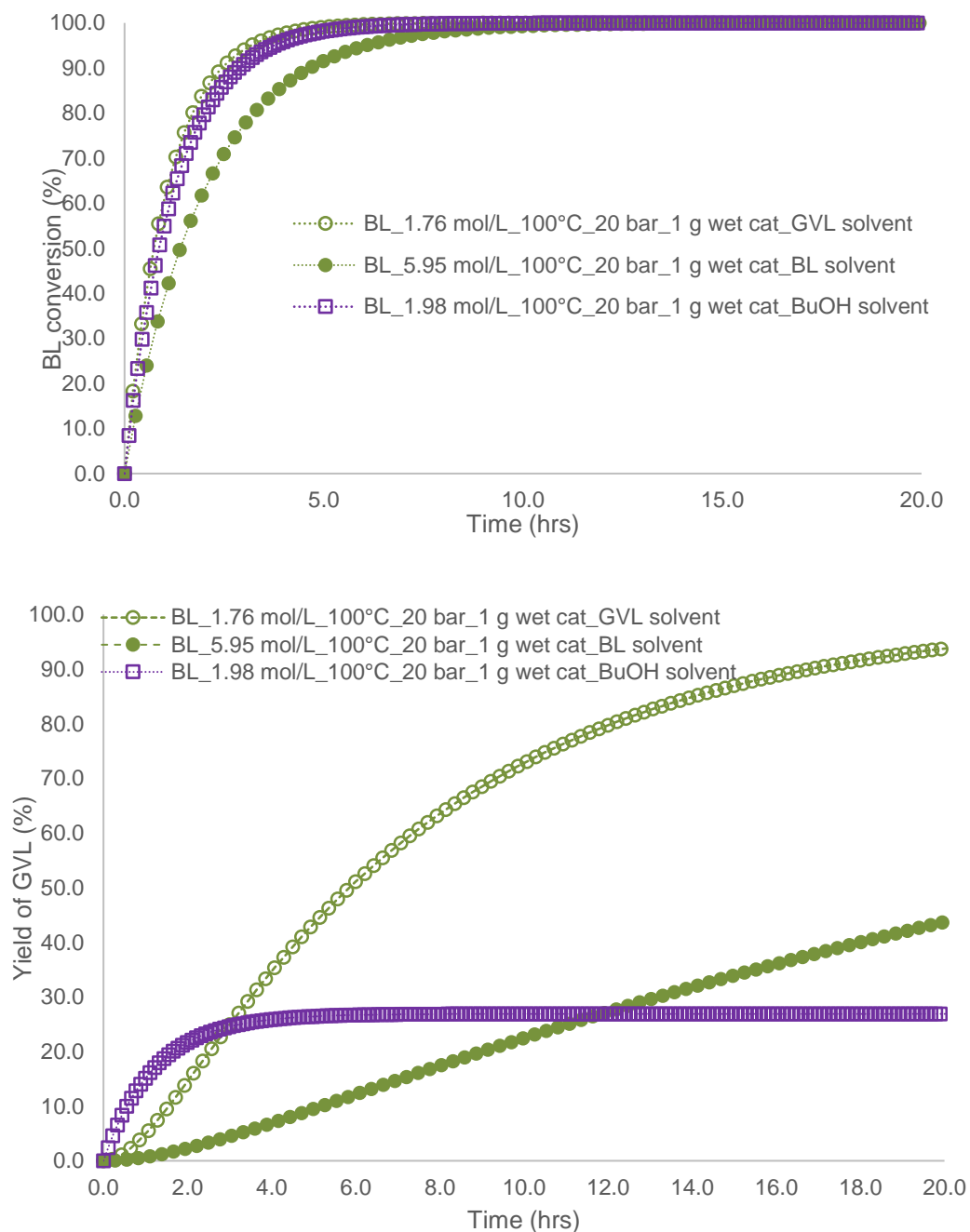
Parameters	Units	GVL solvent	BL solvent	BuOH solvent
$k_1(T = 378.15K)$	$L \text{ mol}^{-1} \text{ s}^{-1} \text{ kg(dry basis cat)}^{-1}$	$1.429 \pm 0.222$	$0.63 \pm 0.07$	$1.76 \pm 0.001$
$E_{a1}$	$J \text{ mol}^{-1}$	$21450.530 \pm 11950.000$	$25365.86 \pm 20640.00$	$178006.60 \pm 166.50$
$k_2(T = 378.15K)$	$s^{-1}$	$4.974 \cdot 10^{-05} \pm 7.001 \cdot 10^{-05}$	$1.28 \cdot 10^{-05} \pm 9.08 \cdot 10^{-07}$	$3013.30 \pm 0.52$
$E_{a2}$	$J \text{ mol}^{-1}$	$45908.800 \pm 15840.000$	$84877.11 \pm 15430.00$	$16442.14 \pm 71.98$
K	$\text{mol L}^{-1}$	-	-	$2.62 \pm 0.48$

From the estimated rate constants (Table 7), it is possible to calculate the evolution of the rate constants versus time (Figs 9). One can notice that when the reaction temperature is higher than 105°C, the kinetics of hydrogenation and cyclization steps in butanol are the highest (Figs 9). The rate constants in BL solvent are the lowest ones.



**Figs 9.** Rate constants versus temperature.

In order to have a better overview, the kinetic simulation of Exps 2, 4 and 6 was carried on long reaction time (Figs 10). Figs 10 confirm that the kinetics in the BuOH solvent is faster, but for the cyclization reaction in the BuOH solvent the reverse reaction is not negligible, limiting the GVL production.



Figs 10. BL conversion and GVL yield at 100°C and 20 bars in GVL, BL and BuOH solvents (same initial conditions than Exps 2, 4 and 6).

Due to the values of butanol vapor pressure when the temperature is higher than 110°C, it was deemed reasonable to perform a kinetic comparison within the temperature range 100-110°C. The kinetics of both reaction steps is faster in butanol solvent when the reaction temperature is higher than 105°C; however, the reverse reaction for the cyclization step is not negligible, limiting the GVL production.

#### 4. Conclusion

The interest in the production of  $\gamma$ -valerolactone (GVL) from the hydrogenation of levulinic acid or alkyl levulinates is increasing. This molecule is produced from second-generation biomass and it is a platform molecule. In this study, the solvent effect on the kinetics of GVL production from the hydrogenation of n-butyl levulinate (BL) over Ru/C was evaluated. Three solvents were tested: GVL, a reaction product, BL, a reactant and butanol, a reaction co-product.

Kinetic experiments were carried out in an autoclave under isobaric condition at 20 bar and under isothermal condition. Based on the evolution of vapor pressure with temperature for the three solvents, reaction temperatures that cause low vapor pressure, i.e., less than 1 bar, were selected. For this reason, kinetic experiments in GVL, in BL and in butanol were performed within the temperature ranges 100-120°C, 100-110°C and 100-110°C, respectively. The catalyst amount was varied between 0.0005 and 0.001 kg wet basis.

From PC-SAFT, it was found that the hydrogen solubility in these solvents at 20 bar of hydrogen and within the temperature range 100-120°C increase in the following order:  $H_2$  solubility/Butanol solvent >  $H_2$  solubility/BL > solvent  $H_2$  solubility/GVL solvent. Based on PC-SAFT, it was possible to estimate the values of hydrogen concentration in the liquid phase at different reaction times. This information was fundamental to the kinetic modeling stage.

A kinetic model was developed for each solvents using a Bayesian approach. This reaction system comprises two reaction steps: hydrogenation and cyclization. From the experimental observation, when butanol is used as a solvent, the reverse reaction for the cyclization step is not negligible. The rate equation for each step was expressed

using the power-law approach. From the kinetic models, it was found that the kinetics of hydrogenation and cyclization steps are faster in butanol solvent for reaction temperature higher than 105°C, but the reversibility of the second step limits the production of GVL. At 100°C and 20 bar of hydrogen, it was found that after 15 hours of reaction time, the GVL yields were 27% in butanol, 34% in BL and 87% in GVL.

By combining the evolution of vapor pressure, hydrogen solubility, the kinetics of both reaction and the reversibility of this reaction system, the use of GVL solvent is better for the hydrogenation of n-butyl levulinate to GVL.

## Notation

$a^{assoc}$	Association contribution
$a^{disp}$	Dispersion contribution
$a^{hc}$	Hard-chain contribution
$a^{res}$	Residual Helmholtz energy
Ea	Activation energy [J.mol <sup>-1</sup> ]
$f_{iu}(\xi_u, \theta)$	Estimated value for the response $i$
K	Equilibrium constant
k	Rate constant
k <sub>B</sub>	Boltzmann constant
$m_{seg}$	Segment number
P	Pressure [bar]
R	Gas constant [J.(K.mol) <sup>-1</sup> ]
R <sub>i</sub>	Reaction rate $i$
$S(\theta)$	Objective function
T <sub>R</sub>	Temperature of the reaction mixture [°C]
T <sub>Ref</sub>	Reference temperature [°C]
V <sub>liq</sub>	Volume of liquid [L]
$y_i$	Mole fraction of the component $i$ in the vapor phase
$Y_{iu}$	Experimental concentration

## Greek letters

$\varepsilon^{AiBi}$	Association-energy parameter
$\kappa^{AiBi}$	Association-volume parameter

$\mu_i^{\text{res}}$	Residual chemical potential
$\rho$	Mass density [kg.m <sup>-3</sup> ]
$ v(\theta) $	Determinant of the covariance matrix of the responses
$\sigma_i$	Segment diameter
$u_i/k_B$	Dispersion-energy parameter
$\varphi_{0i}^L$	Fugacity coefficient of the pure component in the liquid phase
$\varphi_i^L$	Fugacity coefficient of the component in the liquid phase
$\omega_{\text{cat.}}$	Catalyst loading [kg.m <sup>-3</sup> ]

### Subscripts and superscripts

Ref	reference
*	interfacial value

### Abbreviations

BL	n-butyl levulinate
BuOH	butanol
Int	Intermediate
GVL	$\gamma$ -valerolactone

## **Acknowledgements**

This study has been done in the framework of Task 2: “Green process: 2<sup>nd</sup> generation of biomass” of AMED project. The authors thank the AMED project. The AMED project has been funded with the support from the European Union with the European Regional Development Fund (ERDF) and from the Regional Council of Normandie. The authors thank the *Maîtrise des Risques et Environnementaux* department, and the Erasmus programme to make the research project of Sarah Capecci possible.

## References

- Al-Shaal, M.G., Wright, W.R.H., Palkovits, R., 2012. Exploring the ruthenium catalysed synthesis of  $\gamma$ -valerolactone in alcohols and utilisation of mild solvent-free reaction conditions. *Green Chem.* 14, 1260–1263. <https://doi.org/10.1039/C2GC16631C>
- Alonso, D.M., Wettstein, S.G., Dumesic, J.A., 2013. Gamma-valerolactone, a sustainable platform molecule derived from lignocellulosic biomass. *Green Chem.* 15, 584–595. <https://doi.org/10.1039/C3GC37065H>
- Altuntepe, E., Emel'yanenko, V.N., Forster-Rotgers, M., Sadowski, G., Verevkin, S.P., Held, C., 2017. Thermodynamics of enzyme-catalyzed esterifications: II. Levulinic acid esterification with short-chain alcohols. *Appl. Microbiol. Biotechnol.* 101, 7509–7521. <https://doi.org/10.1007/s00253-017-8481-4>
- Ariba, H., Wang, Y., Devouge-Boyer, C., Stateva, R.P., Leveneur, S., 2020. Physicochemical properties for the reaction systems: levulinic acid, its esters, and  $\gamma$ -valerolactone. *J. Chem. Eng. Data* 65, 3008–3020. <https://doi.org/10.1021/acs.jced.9b00965>
- Berthelot, D., 1898. Sur le mélange des gaz. *Comptes rendus l'Académie des Sci.* 126, 1703–1706.
- Caracotsios, M., Stewart, W.E., 1985. Sensitivity analysis of initial value problems with mixed odes and algebraic equations. *Comput. Chem. Eng.* 9, 359–365. [https://doi.org/10.1016/0098-1354\(85\)85014-6](https://doi.org/10.1016/0098-1354(85)85014-6)
- Chandel, A.K., Garlapati, V.K., Jeevan Kumar, S.P., Hans, M., Singh, A.K., Kumar, S., 2020. The role of renewable chemicals and biofuels in building a bioeconomy. *Biofuels, Bioprod. Biorefining* 14(4), 830-844. <https://doi.org/10.1002/bbb.2104>
- Chew, A.K., Walker, T.W., Shen, Z., Demir, B., Witteman, L., Euclide, J., Huber, G.W., Dumesic, J.A., Van Lehn, R.C., 2020. Effect of Mixed-Solvent Environments on

- the Selectivity of Acid-Catalyzed Dehydration Reactions. *ACS Catal.* 10, 1679–1691. <https://doi.org/10.1021/acscatal.9b03460>
- Chia, M., Dumesic, J.A., 2011. Liquid-phase catalytic transfer hydrogenation and cyclization of levulinic acid and its esters to  $\gamma$ -valerolactone over metal oxide catalysts. *Chem. Commun.* 47, 12233–12235. <https://doi.org/10.1039/C1CC14748J>
- Deng, L., Li, J., Lai, D.-M., Fu, Y., Guo, Q.-X., 2009. Catalytic conversion of biomass-derived carbohydrates into  $\gamma$ -valerolactone without using an external H<sub>2</sub> supply. *Angew. Chemie Int. Ed.* 48, 6529–6532. <https://doi.org/10.1002/anie.200902281>
- Deng, L., Zhao, Y., Li, J., Fu, Y., Liao, B., Guo, Q.-X., 2010. Conversion of levulinic acid and formic acid into  $\gamma$ -valerolactone over heterogeneous catalysts. *ChemSusChem* 3, 1172–1175. <https://doi.org/10.1002/cssc.201000163>
- Du, X.-L., He, L., Zhao, S., Liu, Y.-M., Cao, Y., He, H.-Y., Fan, K.-N., 2011. Hydrogen-independent reductive transformation of carbohydrate biomass into  $\gamma$ -valerolactone and pyrrolidone derivatives with supported gold catalysts. *Angew. Chemie Int. Ed.* 50, 7815–7819. <https://doi.org/10.1002/anie.201100102>
- Du, X., Liu, Y., Wang, J., Cao, Y., Fan, K., 2013. Catalytic conversion of biomass-derived levulinic acid into  $\gamma$ -valerolactone using iridium nanoparticles supported on carbon nanotubes. *Chinese J. Catal.* 34, 993–1001. [https://doi.org/10.1016/S1872-2067\(11\)60522-6](https://doi.org/10.1016/S1872-2067(11)60522-6)
- Dutta, S., De, S., Saha, B., 2012. A brief summary of the synthesis of polyester building-block chemicals and biofuels from 5-hydroxymethylfurfural. *Chempluschem* 77, 259–272. <https://doi.org/10.1002/cplu.201100035>
- Enumula, S.S., Gurram, V.R.B., Kondeboina, M., Burri, D.R., Kamaraju, S.R.R., 2016. ZrO<sub>2</sub>/SBA-15 as an efficient catalyst for the production of  $\gamma$ -valerolactone from

- biomass-derived levulinic acid in the vapour phase at atmospheric pressure. *RSC Adv.* 6, 20230–20239. <https://doi.org/10.1039/C5RA27513J>
- Fábos, V., Mika, L.T., Horváth, I.T., 2014. Selective conversion of levulinic and formic acids to  $\gamma$ -valerolactone with the shvo catalyst. *Organometallics* 33, 181–187. <https://doi.org/10.1021/om400938h>
- Fellay, C., Dyson, P.J., Laurenczy, G., 2008. A viable hydrogen-storage system based on selective formic acid decomposition with a ruthenium catalyst. *Angew. Chemie Int. Ed.* 47, 3966–3968. <https://doi.org/10.1002/anie.200800320>
- Feng, X., Tian, Y., Xiao, L., Wu, W., 2020. Fe–Mo<sub>2</sub>C: A magnetically recoverable catalyst for hydrogenation of ethyl levulinate into  $\gamma$ -valerolactone. *Catal. Letters* 150, 2027–2037. <https://doi.org/10.1007/s10562-020-03124-z>
- Ge, X., Chang, C., Zhang, L., Cui, S., Luo, X., Hu, S., Qin, Y., Li, Y., 2018. Conversion of lignocellulosic biomass into platform chemicals for biobased polyurethane application. *Advances in Bioenergy* 3, 161-213. <https://doi.org/10.1016/bs.aibe.2018.03.002>
- Gross, J., Sadowski, G., 2002. Application of the perturbed-chain soft equation of state to associating systems. *Ind. Eng. Chem. Res.* 41, 5510–5515. <https://doi.org/10.1021/ie010954d>
- Gross, J., Sadowski, G., 2001. Perturbed-Chain SAFT: An equation of state based on a perturbation theory for chain molecules. *Ind. Eng. Chem. Res.* 40, 1244–1260. <https://doi.org/10.1021/ie0003887>
- He, J., Li, H., Lu, Y.-M., Liu, Y.-X., Wu, Z.-B., Hu, D.-Y., Yang, S., 2016. Cascade catalytic transfer hydrogenation–cyclization of ethyl levulinate to  $\gamma$ -valerolactone with Al–Zr mixed oxides. *Appl. Catal. A Gen.* 510, 11–19. <https://doi.org/10.1016/j.apcata.2015.10.049>

- Heeres, H., Handana, R., Chunai, D., Rasrendra, C.B., Girisuta, B., Heeres, H.J., 2009. Combined dehydration/(transfer)-hydrogenation of C6-sugars (D-glucose and D-fructose) to  $\gamma$ -valerolactone using ruthenium catalysts. *Green Chem.* 11, 1247–1255. <https://doi.org/10.1039/B904693C>
- Hengne, A.M., Malawadkar, A. V, Biradar, N.S., Rode, C. V, 2014. Surface synergism of an Ag–Ni/ZrO<sub>2</sub> nanocomposite for the catalytic transfer hydrogenation of bio-derived platform molecules. *RSC Adv.* 4, 9730–9736. <https://doi.org/10.1039/C3RA46495D>
- Hengne, A.M., Rode, C. V, 2012. Cu–ZrO<sub>2</sub> nanocomposite catalyst for selective hydrogenation of levulinic acid and its ester to  $\gamma$ -valerolactone. *Green Chem.* 14, 1064–1072. <https://doi.org/10.1039/C2GC16558A>
- Hengst, K., Schubert, M., Carvalho, H.W.P., Lu, C., Kleist, W., Grunwaldt, J.-D., 2015. Synthesis of  $\gamma$ -valerolactone by hydrogenation of levulinic acid over supported nickel catalysts. *Appl. Catal. A Gen.* 502, 18–26. <https://doi.org/10.1016/j.apcata.2015.05.007>
- Horváth, I.T., Mehdi, H., Fábos, V., Boda, L., Mika, L.T., 2008.  $\gamma$ -Valerolactone—a sustainable liquid for energy and carbon-based chemicals. *Green Chem.* 10, 238–242. <https://doi.org/10.1039/B712863K>
- Isikgor, F.H., Becer, C.R., 2015. Lignocellulosic biomass: a sustainable platform for the production of bio-based chemicals and polymers. *Polym. Chem.* 6, 4497–4559. <https://doi.org/10.1039/C5PY00263J>
- Kasar, G.B., Date, N.S., Bhosale, P.N., Rode, C. V, 2018. Steering the ester and  $\gamma$ -valerolactone selectivities in levulinic acid hydrogenation. *Energy & Fuels* 32, 6887–6900. <https://doi.org/10.1021/acs.energyfuels.8b01263>
- Klajmon, M., Řehák, K., Morávek, P., Matoušová, M., 2015. Binary liquid–liquid

- equilibria of  $\gamma$ -valerolactone with some hydrocarbons. *J. Chem. Eng. Data* 60, 1362–1370. <https://doi.org/10.1021/je501074b>
- Kohli, K., Prajapati, R., Sharma, B.K., 2019. Bio-based chemicals from renewable biomass for integrated biorefineries. *Energies* 12, 233. <https://doi.org/10.3390/en12020233>
- Kuwahara, Y., Kaburagi, W., Osada, Y., Fujitani, T., Yamashita, H., 2017. Catalytic transfer hydrogenation of biomass-derived levulinic acid and its esters to  $\gamma$ -valerolactone over  $ZrO_2$  catalyst supported on SBA-15 silica. *Catal. Today* 281, 418–428. <https://doi.org/10.1016/j.cattod.2016.05.016>
- Li, H., Fang, Z., Yang, S., 2016a. Direct catalytic transformation of biomass derivatives into biofuel component  $\gamma$ -valerolactone with magnetic nickel–zirconium nanoparticles. *Chempluschem* 81, 135–142. <https://doi.org/10.1002/cplu.201500492>
- Li, H., Fang, Z., Yang, S., 2016b. Direct conversion of sugars and ethyl levulinate into  $\gamma$ -valerolactone with superparamagnetic acid–base bifunctional zrfeox nanocatalysts. *ACS Sustain. Chem. Eng.* 4, 236–246. <https://doi.org/10.1021/acssuschemeng.5b01480>
- Lin, H., Chen, J., Zhao, Y., Wang, S., 2017. Conversion of C5 carbohydrates into furfural catalyzed by so<sub>3</sub>h-functionalized ionic liquid in renewable  $\gamma$ -valerolactone. *Energy & Fuels* 31, 3929–3934. <https://doi.org/10.1021/acs.energyfuels.6b01975>
- Liu, C., Wei, M., Wang, J., Xu, J., Jiang, J., Wang, K., 2020. Facile directional conversion of cellulose and bamboo meal wastes over low-cost sulfate and polar aprotic solvent. *ACS Sustain. Chem. Eng.* 8, 5776–5786. <https://doi.org/10.1021/acssuschemeng.0c01280>
- Lorentz, H.A., 1881. Ueber die Anwendung des Satzes vom Virial in der kinetischen

- Theorie der Gase. *Ann. Phys.* 248, 127–136.  
<https://doi.org/10.1002/andp.18812480110>
- Luo, W., Deka, U., Beale, A.M., van Eck, E.R.H., Bruijninx, P.C.A., Weckhuysen, B.M., 2013. Ruthenium-catalyzed hydrogenation of levulinic acid: Influence of the support and solvent on catalyst selectivity and stability. *J. Catal.* 301, 175–186.  
<https://doi.org/10.1016/j.jcat.2013.02.003>
- Luterbacher, J.S., Alonso, D.M., Dumesic, J.A., 2014. Targeted chemical upgrading of lignocellulosic biomass to platform molecules. *Green Chem.* 16, 4816–4838.  
<https://doi.org/10.1039/C4GC01160K>
- Manzer, L.E., 2004. Catalytic synthesis of  $\alpha$ -methylene- $\gamma$ -valerolactone: a biomass-derived acrylic monomer. *Appl. Catal. A Gen.* 272, 249–256.  
<https://doi.org/10.1016/j.apcata.2004.05.048>
- Mehdi, H., Fábos, V., Tuba, R., Bodor, A., Mika, L.T., Horváth, I.T., 2008. Integration of homogeneous and heterogeneous catalytic processes for a multi-step conversion of biomass: from sucrose to levulinic acid,  $\gamma$ -valerolactone, 1,4-pentanediol, 2-methyl-tetrahydrofuran, and alkanes. *Top. Catal.* 48, 49–54.  
<https://doi.org/10.1007/s11244-008-9047-6>
- Merklein, K., Fong, S.S., Deng, Y., 2016. Biomass Utilization, in: *Biotechnology for Biofuel Production and Optimization*. pp. 291–324. <https://doi.org/10.1016/B978-0-444-63475-7.00011-X>
- Negahdar, L., Al-Shaal, M.G., Holzhäuser, F.J., Palkovits, R., 2017. Kinetic analysis of the catalytic hydrogenation of alkyl levulinates to  $\gamma$ -valerolactone. *Chem. Eng. Sci.* 158, 545–551. <https://doi.org/10.1016/j.ces.2016.11.007>
- Ortiz-Cervantes, C., García, J.J., 2013. Hydrogenation of levulinic acid to  $\gamma$ -valerolactone using ruthenium nanoparticles. *Inorganica Chim. Acta* 397, 124–

128. <https://doi.org/10.1016/j.ica.2012.11.031>

- Park, J.Y., Kim, M.A., Lee, S.J., Jung, J., Jang, H.M., Upare, P.P., Hwang, Y.K., Chang, J.-S., Park, J.K., 2015. Preparation and characterization of carbon-encapsulated iron nanoparticles and their catalytic activity in the hydrogenation of levulinic acid. *J. Mater. Sci.* 50, 334–343. <https://doi.org/10.1007/s10853-014-8592-6>
- Piskun, A.S., van de Bovenkamp, H.H., Rasrendra, C.B., Winkelman, J.G.M., Heeres, H.J., 2016. Kinetic modeling of levulinic acid hydrogenation to  $\gamma$ -valerolactone in water using a carbon supported Ru catalyst. *Appl. Catal. A Gen.* 525, 158–167. <https://doi.org/10.1016/j.apcata.2016.06.033>
- Pokorný, V., Štejfa, V., Fulem, M., Červinka, C., Růžička, K., 2017. Vapor pressures and thermophysical properties of ethylene carbonate, propylene carbonate,  $\gamma$ -valerolactone, and  $\gamma$ -butyrolactone. *J. Chem. Eng. Data* 62, 4174–4186. <https://doi.org/10.1021/acs.jced.7b00578>
- Qi, L., Horváth, I.T., 2012. Catalytic conversion of fructose to  $\gamma$ -valerolactone in  $\gamma$ -valerolactone. *ACS Catal.* 2, 2247–2249. <https://doi.org/10.1021/cs300428f>
- Ruppert, A.M., Jędrzejczyk, M., Sneka-Płatek, O., Keller, N., Dumon, A.S., Michel, C., Sautet, P., Grams, J., 2016. Ru catalysts for levulinic acid hydrogenation with formic acid as a hydrogen source. *Green Chem.* 18, 2014–2028. <https://doi.org/10.1039/C5GC02200B>
- Safarov, J., Ahmadov, B., Mirzayev, S., Shahverdiyev, A., Hassel, E., 2015. Vapor pressures of 1-butanol over wide range of temperatures. *Chemistry* 24, 226–246.
- Shimizu, K., Kanno, S., Kon, K., 2014. Hydrogenation of levulinic acid to  $\gamma$ -valerolactone by Ni and MoO<sub>x</sub> co-loaded carbon catalysts. *Green Chem.* 16, 3899–3903. <https://doi.org/10.1039/C4GC00735B>

- Shuai, L., Luterbacher, J., 2016. Organic solvent effects in biomass conversion reactions. *ChemSusChem* 9, 133–155. <https://doi.org/10.1002/cssc.201501148>
- Son, P.A., Nishimura, S., Ebitani, K., 2014. Production of  $\gamma$ -valerolactone from biomass-derived compounds using formic acid as a hydrogen source over supported metal catalysts in water solvent. *RSC Adv.* 4, 10525–10530. <https://doi.org/10.1039/C3RA47580H>
- Song, J., Wu, L., Zhou, B., Zhou, H., Fan, H., Yang, Y., Meng, Q., Han, B., 2015a. A new porous Zr-containing catalyst with a phenate group: an efficient catalyst for the catalytic transfer hydrogenation of ethyl levulinate to  $\gamma$ -valerolactone. *Green Chem.* 17, 1626–1632. <https://doi.org/10.1039/C4GC02104E>
- Song, J., Zhou, B., Zhou, H., Wu, L., Meng, Q., Liu, Z., Han, B., 2015b. Porous zirconium–phytic acid hybrid: a highly efficient catalyst for meerwein–ponndorf–verley reductions. *Angew. Chem. Int. Ed.* 54, 9399–9403. <https://doi.org/10.1002/anie.201504001>
- Stewart, W.E., Caracotsios, M., 2010. Athena Visual Studio. URL [www.athenavisual.com](http://www.athenavisual.com) (accessed 6.10.20).
- Stewart, W.E., Caracotsios, M., 2008. *Computer-Aided Modeling of Reactive Systems*, Wiley & So. ed. Wiley & Sons, New Jersey.
- Sudhakar, M., Lakshmi Kantam, M., Swarna Jaya, V., Kishore, R., Ramanujachary, K. V., Venugopal, A., 2014. Hydroxyapatite as a novel support for Ru in the hydrogenation of levulinic acid to  $\gamma$ -valerolactone. *Catal. Commun.* 50, 101–104. <https://doi.org/10.1016/j.catcom.2014.03.005>
- Takkellapati, S., Li, T., Gonzalez, M.A., 2018. An overview of biorefinery-derived platform chemicals from a cellulose and hemicellulose biorefinery. *Clean Technol. Environ. Policy* 20, 1615–1630. <https://doi.org/10.1007/s10098-018-1568-5>

- Tang, X., Hu, L., Sun, Y., Zhao, G., Hao, W., Lin, L., 2013. Conversion of biomass-derived ethyl levulinate into  $\gamma$ -valerolactone via hydrogen transfer from supercritical ethanol over a ZrO<sub>2</sub> catalyst. *RSC Adv.* 3, 10277–10284.  
<https://doi.org/10.1039/C3RA41288A>
- Tang, X., Zeng, X., Li, Z., Hu, L., Sun, Y., Liu, S., Lei, T., Lin, L., 2014. Production of  $\gamma$ -valerolactone from lignocellulosic biomass for sustainable fuels and chemicals supply. *Renew. Sustain. Energy Rev.* 40, 608–620.  
<https://doi.org/10.1016/j.rser.2014.07.209>
- Tang, X., Zeng, X., Li, Z., Li, W., Jiang, Y., Hu, L., Liu, S., Sun, Y., Lin, L., 2015. In situ generated catalyst system to convert biomass-derived levulinic acid to  $\gamma$ -valerolactone. *ChemCatChem* 7, 1372–1379.  
<https://doi.org/10.1002/cctc.201500115>
- Testa, M.L., Corbel-Demilly, L., La Parola, V., Venezia, A.M., Pinel, C., 2015. Effect of Au on Pd supported over HMS and Ti doped HMS as catalysts for the hydrogenation of levulinic acid to  $\gamma$ -valerolactone. *Catal. Today* 257, 291–296.  
<https://doi.org/10.1016/j.cattod.2014.06.009>
- Thi, C. Le, Tamouza, S., Passarello, J.-P., Tobaly, P., de Hemptinne, J.-C., 2006. Modeling phase equilibrium of H<sub>2</sub> + n-alkane and CO<sub>2</sub> + n-alkane binary mixtures using a group contribution statistical association fluid theory equation of state (GC-SAFT-EOS) with a  $k_{ij}$  group contribution method. *Ind. Eng. Chem. Res.* 45, 6803–6810. <https://doi.org/10.1021/ie060424n>
- Thompson, P.B., 2012. The agricultural ethics of biofuels: The food vs. fuel debate. *Agric.* 2, 339–358. <https://doi.org/10.3390/agriculture2040339>
- Wang, Y., Cipolletta, M., Vernières-Hassimi, L., Casson-Moreno, V., Leveneur, S., 2019. Application of the concept of linear free energy relationships to the

- hydrogenation of levulinic acid and its corresponding esters. *Chem. Eng. J.* 374, 822–831. <https://doi.org/10.1016/j.cej.2019.05.218>
- Wettstein, S.G., Alonso, D.M., Chong, Y., Dumesic, J.A., 2012. Production of levulinic acid and gamma-valerolactone (GVL) from cellulose using GVL as a solvent in biphasic systems. *Energy Environ. Sci.* 5, 8199–8203. <https://doi.org/10.1039/C2EE22111J>
- Wright, W.R.H., Palkovits, R., 2012. Development of heterogeneous catalysts for the conversion of levulinic acid to  $\gamma$ -valerolactone. *ChemSusChem* 5, 1657–1667. <https://doi.org/10.1002/cssc.201200111>
- Xu, H., Hu, D., Yi, Z., Wu, Z., Zhang, M., Yan, K., 2019. Solvent tuning the selective hydrogenation of levulinic acid into biofuels over ni-metal organic framework-derived catalyst. *ACS Appl. Energy Mater.* 2, 6979–6983. <https://doi.org/10.1021/acsaem.9b01439>
- Yan, K., Yang, Y., Chai, J., Lu, Y., 2015. Catalytic reactions of gamma-valerolactone: A platform to fuels and value-added chemicals. *Appl. Catal. B Environ.* 179, 292–304. <https://doi.org/10.1016/j.apcatb.2015.04.030>
- Yuan, J., Li, S.-S., Yu, L., Liu, Y.-M., Cao, Y., He, H.-Y., Fan, K.-N., 2013. Copper-based catalysts for the efficient conversion of carbohydrate biomass into  $\gamma$ -valerolactone in the absence of externally added hydrogen. *Energy Environ. Sci.* 6, 3308–3313. <https://doi.org/10.1039/C3EE40857D>